Journal of Alloys and Compounds 505 (2010) 179–182

Contents lists available at ScienceDirect

Journal of Alloys and Compounds

journal homepage: www.elsevier.com/locate/jallcom

Highly corrosion-resistant $Cu_{70}(Ni,Fe,Mn,Cr)_{30}$ cupronickel designed using a cluster model for stable solid solutions

Jie Zhang, Qing Wang, Yingmin Wang, Lishi Wen, Chuang Dong*

Key Lab of Materials Modification by Laser, Ion and Electron Beams, School of Materials Science & Engineering, Dalian University of Technology, Dalian 116024, China

ARTICLE INFO

Article history:
Received 17 February 2010
Accepted 1 June 2010
Available online 12 June 2010

Keywords:
Cu–Ni
Cluster-plus-glue-atom model
Corrosion

ABSTRACT

Minor M (M = Fe, Mn, Cr) additions are widely added to enhance the corrosion resistance of commercial cupronickel alloys. The present paper aims at optimizing the amounts of M in $Cu_{70}(Ni,Fe,Mn,Cr)_{30}$ (at.%) alloys using a cluster-plus-glue-atom model for stable solid solutions. By this model, it assumed that 1 M atom and 12 Ni atoms formed an M-centered and Ni-surrounded cube-octahedron cluster and the isolated M_1Ni_{12} clusters are embedded in a Cu matrix, conforming to a cluster formula $[M_1Ni_{12}]Cu_{30.3} = [M_{1/13}Ni_{12/13}]_{30}Cu_{70}$. A structure of this kind satisfies ideally the nearest neighbor requirement, i.e. only M–Ni and Ni–Cu neighbors are allowed and the unfavorable Cu–M pairs are avoided, and hence it describes a stable solid solution structure with good thermal stability. Electrochemical corrosion measurements indicated that $[(Fe_{0.6}Mn_{0.25}Cr_{0.15})_1Ni_{12}]Cu_{30.3}$ had the best corrosion resistance in 3.5% NaCl aqueous solution.

1. Introduction

Cu–Ni alloys are widely employed as tube and vessel materials due to their excellent resistance to seawater corrosion [1]. The base binary alloys are often alloyed with small amounts of Fe and Mn like UNS C70600 and C71500 alloys which contain 0.5–2.3 wt.% Fe. Minor Fe, Cr and Mn additions are necessary to enhance the corrosion resistance of commercial Cu–Ni alloys [2–4]. Bailey investigated the effect of Fe-addition in a series of Cu–Ni alloys, and found that the presence of visible Fe–Ni precipitates deteriorate the corrosion performance when the Fe content exceeds 2 at.% in the Cu–10Ni alloy (10 wt.%Ni) due to precipitation of a Ni–Fe phase [5,6]. The addition of minor Cr to Cu–Ni was found to be particularly beneficial to enhance the corrosion resistance [7]. Although much research has been devoted to the corrosion behavior of Cu–Ni alloys in seawater, the composition optimum of modification element contents with Fe, Cr and Mn additions in Cu–Ni alloys remain unresolved. Generally, single-phase homogeneous solid solution alloys are desirable for good corrosion resistance performance. Such a single-phase state is easily retained by quenching when the solid solution alloy has the maximum thermal stability. Therefore, the amounts of modification element additions are determined by the stability issue of the Cu–Ni alloys.

In an alloy, the constituent elements showing negative enthalpies of mixing ($\Delta H < 0$) tend to form dissimilar atomic pairs. The local atomic environments of this alloys is characterized by short-range orders, or atomic clusters. We used the atomic cluster structures (1st-neighbor coordination polyhedron clusters) of known crystals to explore the composition rules of bulk metallic glasses and quasicrystals [8,9]. For instance, a Cu-centered Cu_8Zr_5 icosahedron, derived from the Cu_8Zr_3 phase, was used to explain Cu–Zr-based bulk metallic glasses. We proposed a simple and universal composition formula $[cluster]_1(glue\ atom)_x$, $x = 1, 3$. This cluster-based description, termed the cluster-plus-glue-atom model, actually suggests a new way of understanding atomic structures: the Cu_8Zr_5-based glassy structures can be viewed as a random and dense packing of Cu_8Zr_5 icosahedra glued with a third element situated in the interstitial sites between the icosahedral clusters.

This idea can be generalized to those solid solutions composed of metals having negative enthalpies of mixing. In such cases a solute atom should be preferentially surrounded by the solvent ones. The framework of the solid solution structure thereby can be viewed as packings of solute-centered and solvent-surrounded clusters. For the Cu–Ni–Fe alloy system, Fe–Ni dissimilar bonding is preferred against Fe–Fe and Ni–Ni ones in the Fe–Ni FCC solid solutions, which promotes the Fe–Ni-type short-range order. In the ideal case, an Fe atom would be screened completely by 12 solvent Ni atoms, forming cube-octahedron $FeNi_{12}$, and these isolated Fe_1Ni_{12} clusters are embedded in the Cu matrix conforming to a cluster formula $[Fe_1Ni_{12}]Cu_x$ [10]. The Fe(Mn)-modified $Cu_{70}Ni_{30}$ alloy is $[M_{1/13}Ni_{12/13}]_{30}Cu_{70}$ using a cluster-based solid solution model($M = Fe_{1-x}Mn_x$), and the $(Fe_{0.75}Mn_{0.25})_1Ni_{12}]Cu_{30.3}$ has the best corrosion resistance in 3.5% NaCl aqueous solution [11].

* Corresponding author. Tel.: +86 411 84708389; fax: +86 411 84708389.
E-mail address: dong@dlut.edu.cn (C. Dong).

0925-8388/$ – see front matter © 2010 Elsevier B.V. All rights reserved.
doi:10.1016/j.jallcom.2010.06.023

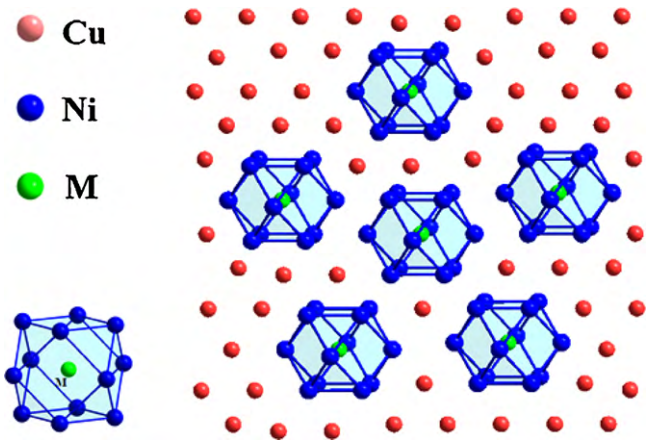

Fig. 1. Cluster-plus-glue-atom model of $[M_1Ni_{12}]Cu_x$ stable solid solution [10].

Using the stable solid solution cluster structure model, the corrosion resistance of $[(Fe_{0.75-x}Mn_{0.25}Cr_x)Ni_{12}]Cu_{30.3}$ alloys with varying Cr additions is addressed in the present paper.

2. Cluster model for FCC solid solution

In Cu–Ni–(Fe, Ni, Cr) solid solution alloys, to reach the maximum stability as required by the enthalpies of mixing between the alloying elements [12], the total amount of Fe, Mn and Cr elements with respect to Ni should be 1:12 as already discussed [10,11] because these elements all have negative enthalpies of mixing with Ni and positive enthalpies of mixing with Cu, i.e. 1 M (M = Fe, Ni and Cr) atom and 12 Ni atoms form a M-centered and Ni-surrounded cube-octahedron M_1Ni_{12} cluster, and these isolated M_1Ni_{12} clusters are embedded in the Cu matrix as shown in Fig. 1. The resultant structure is described by a cluster formula $[M_1Ni_{12}]Cu_x = [M_{1/13}Ni_{12/13}]_{1/(1+x)}Cu_{x/(1+x)}$. Further additions of M would destroy the array of isolated MNi_{12} atomic clusters by forming Ni–M–Ni–M-type long-range orders that eventually lead to precipitation of a Ni-rich intermetallic phase. The solubility of M in the Cu-based solid solution alloy is therefore determined by Ni. The stable solid solution composition of the M-modified $Cu_{70}Ni_{30}$ alloys is derived to be $[M_{1/13}Ni_{12/13}]_{30}Cu_{70} = Cu_{70}Ni_{27.7}M_{2.3}$, or in a simpler cluster formula $[M_1Ni_{12}]Cu_{30.3}$.

3. Experimental procedures

3.1. Materials preparation

The M-modified $Cu_{70}Ni_{30}$ alloy ingots with different Cr addition were prepared by arc melting in a water-chilled copper crucible under pure argon atmosphere. The metal purities were all 99.99 wt.%. The initial vacuum level in the melting chamber was about 5×10^{-3} Pa. To remove solidification segregation, the ingots were annealed for 5 h at 800 ± 5 °C in a vacuum furnace, and subsequently quenched in water. For simplification, a cluster formula $[(Fe_{0.75-x}Mn_{0.25}Cr_x)Ni_{12}]Cu_{30.3}$, is used in the following, where the composition in the bracket corresponds to the Ni–M cluster. The compositions are summarized in Table 1.

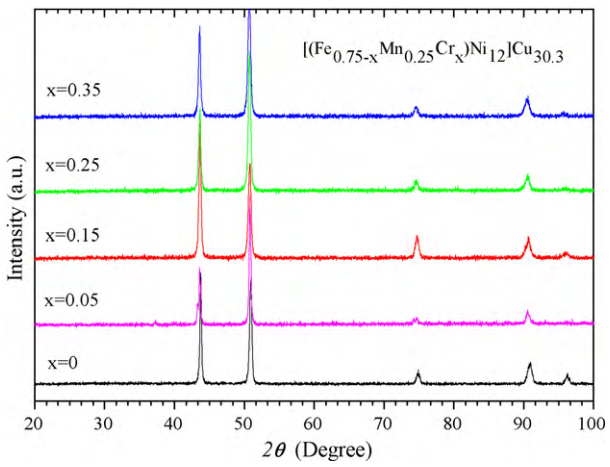

Fig. 2. XRD patterns of the $[(Fe_{0.75-x}Mn_{0.25}Cr_x)Ni_{12}]Cu_{30.3}$ alloys after solution treated and water quenched.

3.2. Materials characterization

Phase identification was carried out by means of X-ray diffraction (Cu-K_α radiation, $\lambda = 0.15406$ nm). Corrosion resistances in a 3.5% NaCl solution were measured to simulate the sea water corrosion. Electrochemical measurements were performed in a typical three-electrode electrochemical cell with saturated calomel as the reference electrode and a platinum sheet as the counter electrode at room temperature. The weight loss method was used to evaluate the general corrosion behavior. Samples for immersion test were first ground with SiC papers and then polished. The as-polished samples were ultrasonically cleaned for the subsequent weight loss tests. The samples were immersed in a 3.5% NaCl solution at room temperature for different durations. The sample weights before and after corrosion were measured within an accuracy of $\pm 5 \times 10^{-4}$ g. Corrosion rates were evaluated by the weight loss per unit mass for a given length of time.

4. Results and discussions

4.1. X-ray diffraction

Fig. 2 shows the XRD patterns of the $[(Fe_{0.75-x}Mn_{0.25}Cr_x)Ni_{12}]Cu_{30.3}$ ($x = 0$, 0.05, 0.15, 0.25 and 0.35), all after annealing at 800 °C for 5 h, and subsequently quenched in water. The XRD patterns can all be indexed by an FCC phase. As compared with the diffraction peak positions of pure Cu metal, the peaks of these solid solution alloys shift to higher diffraction angles, indicating solid solution of small-size Fe, Mn, Cr and Ni in the Cu matrix (Goldschmidt atomic radii of Cu, Ni, Fe, Mn and Cr are 0.128, 0.125, 0.127, 0.126 and 0.128 nm, respectively). The lattice constants were carefully measured using silicon powders as the standard reference. Diffraction peaks {1 1 1}, {2 0 0}, {2 2 0} and {3 1 1} were used to calculate the lattice constants. The average lattice constant of the above alloys is 0.3586 nm.

4.2. Corrosion tests

The effect of Cr contents on the corrosion process was investigated in NaCl solution using potentiodynamic polarization. The

Table 1
Compositions of designed $[M_1Ni_{12}]Cu_{30.3}$ alloy ($M = Fe_{0.75-x}Mn_{0.25}Cr_x$), which correspond to (Fe,Mn,Cr)-modified $Cu_{70}Ni_{30}$ alloys.

Cluster formula	Chemical composition (at.%)					Chemical composition (wt.%)				
	Cu	Ni	Fe	Mn	Cr	Cu	Ni	Fe	Mn	Cr
$[(Fe_{0.75}Mn_{0.25})Ni_{12}]Cu_{30.3}$	70	27.69	1.73	0.58	0.00	71.72	26.21	1.56	0.51	0
$[(Fe_{0.7}Mn_{0.25}Cr_{0.05})Ni_{12}]Cu_{30.3}$	70	27.69	1.62	0.58	0.11	71.73	26.21	1.45	0.51	0.10
$[(Fe_{0.6}Mn_{0.25}Cr_{0.15})Ni_{12}]Cu_{30.3}$	70	27.69	1.39	0.58	0.34	71.74	26.21	1.25	0.51	0.29
$[(Fe_{0.5}Mn_{0.25}Cr_{0.25})Ni_{12}]Cu_{30.3}$	70	27.69	1.16	0.58	0.57	71.75	26.22	1.04	0.51	0.48
$[(Fe_{0.4}Mn_{0.25}Cr_{0.35})Ni_{12}]Cu_{30.3}$	70	27.69	0.92	0.58	0.81	71.76	26.22	0.83	0.51	0.68

Table 2
Corrosion parameters obtained by fitting the curves in Fig. 3.

Cluster formula	E_{corr} (V)	i_{corr} (μA cm^{-2})	β_a (V dec^{-1})	β_c (V dec^{-1})
$[(Fe_{0.75}Mn_{0.25})Ni_{12}]Cu_{30.3}$	−0.123	7.5	0.194	−0.154
$[(Fe_{0.7}Mn_{0.25}Cr_{0.05})Ni_{12}]Cu_{30.3}$	−0.121	6.2	0.194	−0.139
$[(Fe_{0.6}Mn_{0.25}Cr_{0.15})Ni_{12}]Cu_{30.3}$	−0.116	4.7	0.136	−0.115
$[(Fe_{0.5}Mn_{0.25}Cr_{0.25})Ni_{12}]Cu_{30.3}$	−0.122	23.6	0.195	−0.112
$[(Fe_{0.4}Mn_{0.25}Cr_{0.35})Ni_{12}]Cu_{30.3}$	−0.134	43.8	0.172	−0.121

room-temperature potentiodynamic polarization curves of the $[(Fe_{0.75-x}Mn_{0.25}Cr_x)Ni_{12}]Cu_{30.3}$ (x = 0,0.05,0.15,0.25 and 0.35) alloys are presented in Fig. 3. The plots were analyzed by Tafel extrapolation, and the parameters such as corrosion current density (i_{corr}) and corrosion potential (E_{corr}) were calculated and tabulated in Table 2.

Fig. 4 shows the variations of i_{corr} and E_{corr} of $[(Fe_{0.75-x}Mn_{0.25}Cr_x)Ni_{12}]Cu_{30.3}$ stable solid solution alloys as a function of the Cr contents. It is clear that the $[(Fe_{0.75-x}Mn_{0.25}Cr_x)Ni_{12}]Cu_{30.3}$ stable solid solution alloys show a high corrosion resistance, with the lower i_{corr} and the higher E_{corr}. The corrosion current density decreases with the increase of the Cr contents up to x = 0.15, followed by an increasing trend. The Cr addition can improve the corrosion resistance, but more Cr additions negate the corrosion behaviors due to the decrease of Fe content.

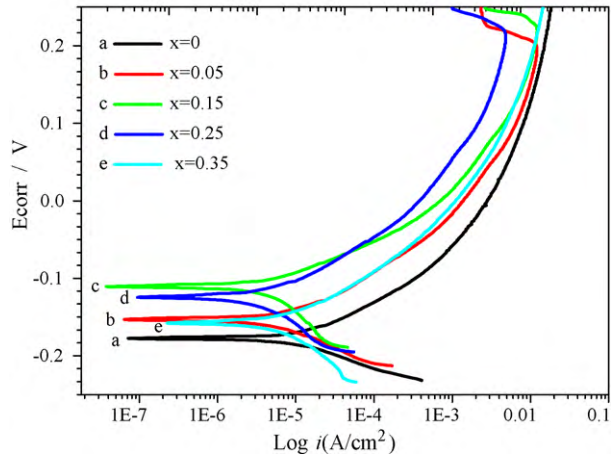

Fig. 3. Comparison of potentiodynamic polarization curves of the $[(Fe_{0.75-x}Mn_{0.25}Cr_x)Ni_{12}]Cu_{30.3}$ alloys in 3.5% NaCl.

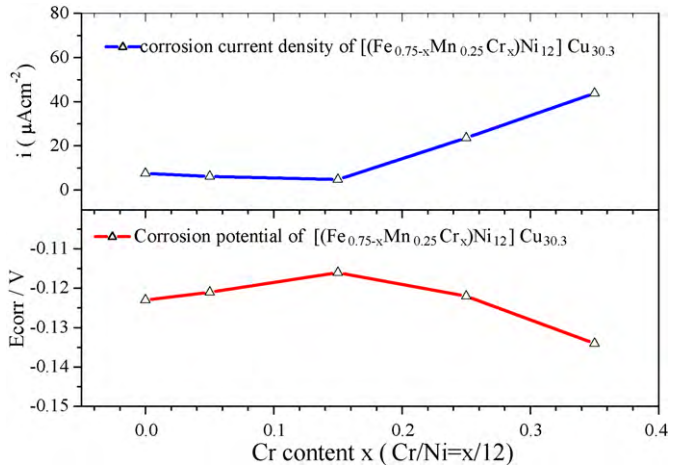

Fig. 4. Variation of corrosion current density (i_{corr}) and corrosion potential (E_{corr}) vs Cr content in $[(Fe_{0.75-x}Mn_{0.25}Cr_x)Ni_{12}]Cu_{30.3}$ alloys.

Therefore, the solid solution $[(Fe_{0.6}Mn_{0.25}Cr_{0.15})Ni_{12}]Cu_{30.3}$ alloy modified by Fe, Mn and Cr addition posses the best corrosion resistance.

To further investigate the effect of the Fe, Mn and Cr content on the corrosion behavior of the $[(Fe_{0.75-x}Mn_{0.25}Cr_x)Ni_{12}]Cu_{30.3}$ (x = 0, 0.05, 0.15, 0.25 and 0.35) alloys, the impedance data for the alloys recorded after 30 min of electrode immersion in 3.5% (wt.%) NaCl solutions under steady state conditions are measured by electrochemical impedance spectroscopy (EIS) and the results are presented as Bode plots in Fig. 5. The Bode plots of the $[(Fe_{0.75-x}Mn_{0.25}Cr_x)Ni_{12}]Cu_{30.3}$ stable solid solution alloys show a major phase maximum at intermediate frequencies and another minor phase maximum at low frequencies.

The experimental impedance data were fitted to theoretical values according to the equivalent circuit model in Fig. 6. The time constant, at high frequencies, is originated from the $R_t - C_d$ combination while at low frequencies, initiated from the $R_f - C_s$ combination. C_d, and a resistor, R_t, in series with a resistor, R_s, representing the solution resistance, the electrode impedance, Z is represented by the mathematical formulation [13,14]: $Z = R_s + Rc/(1 + (2\pi f R_f C_{PE1})^{\alpha})$, where α denotes an empirical parameter ($0 \le \alpha \le 1$) and f is the frequency in Hz. The above relationship is known as the dispersion formula and it takes into account of the deviation from the ideal capacitor C, behavior in terms of a distribution of time constants due to surface inhomogeneties, roughness effects and variations in properties or compositions of surface layers.

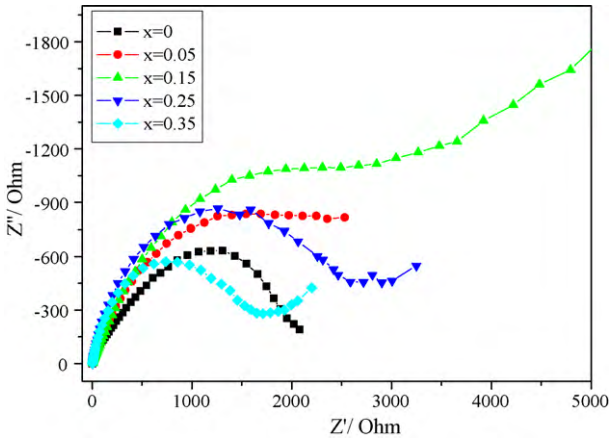

Fig. 5. Nyquist and Bode plots for $[(Fe_{0.75-x}Mn_{0.25}Cr_x)Ni_{12}]Cu_{30.3}$ alloys exposed to 3.5% NaCl solution.

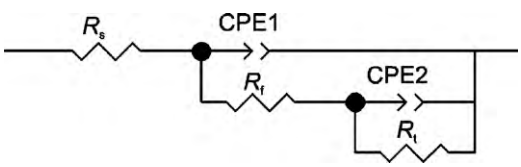

Fig. 6. Equivalent circuit model for fitting the experimental impedance data of $[(Fe_{0.75-x}Mn_{0.25}Cr_x)Ni_{12}]Cu_{30.3}$ alloys.

Table 3
Electrochemical impedance parameters of $[(Fe_{0.75-x}Mn_{0.25}Cr_x)Ni_{12}]Cu_{30.3}$.

Alloy series	Rs (Ω cm^2)	CPE1 (μF cm^{-2})	α_1	Rf (Ω cm^2)	CPE2 (μF cm^{-2})	α_2	Rt (kΩ cm^2)
$[(Fe_{0.75}Mn_{0.25})Ni_{12}]Cu_{30.3}$	2.37	0.22	0.79	861	2.25	0.92	208
$[(Fe_{0.7}Mn_{0.25}Cr_{0.05})Ni_{12}]Cu_{30.3}$	4.54	0.20	0.84	2144	2.09	0.59	715
$[(Fe_{0.6}Mn_{0.25}Cr_{0.15})Ni_{12}]Cu_{30.3}$	3.15	0.14	0.63	2272	1.48	0.92	844
$[(Fe_{0.5}Mn_{0.25}Cr_{0.25})Ni_{12}]Cu_{30.3}$	2.98	0.26	0.83	1681	1.85	0.89	458
$[(Fe_{0.4}Mn_{0.25}Cr_{0.35})Ni_{12}]Cu_{30.3}$	2.01	0.27	0.81	1043	1.78	0.88	240

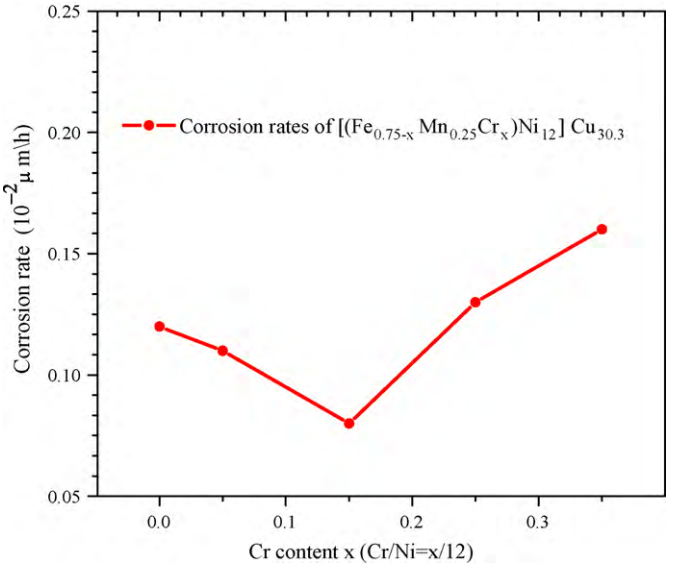

Fig. 7. Static immersion corrosion rates as a function of Cr content x in the $[(Fe_{0.75-x}Mn_{0.25}Cr_x)Ni_{12}]Cu_{30.3}$ alloys after solution treated and water quenched.

The calculated electrochemical impedance parameters for $[(Fe_{0.75-x}Mn_{0.25}Cr_x)Ni_{12}]Cu_{30.3}$ alloy with different Cr contents are summarized in Table 3. The recorded impedance data show a decrease in the impedance values with increasing the Cr content up to $x = 0.15$. Further increase of the Cr content leads to an increase in the impedance values. The results show that the increase of the Cr contents increases the impedance values of the alloy, which indicates that the stability of the alloy increases. The incensement of the Cr contents in $[(Fe_{0.75-x}Mn_{0.25}Cr_x)Ni_{12}]Cu_{30.3}$ has no significant effect on the passive film thickness. A critical Cr content blow $x = 0.15$ is necessary for the Cu–Ni alloys stability. Above $x = 0.15$ both the surface film resistance and thickness increase and the alloys show better stability. The results reveal that the corrosion process is diffusion-controlled. The corrosion behavior of the alloys after long immersion time in the NaCl solution is controlled by the passivating properties of modified elements, and hence the corrosion current density decreases as the Cr content increases.

Fig. 7 shows the static immersion corrosion rates of $[(Fe_{0.75-x}Mn_{0.25}Cr_x)Ni_{12}]Cu_{30.3}$ ($x = 0$, 0.05, 0.15, 0.25 and 0.35) stable solid solution alloys with the Cr additions exposed to the 3.5% NaCl solution for 240 h. It is clear that the Cr addition can further improve the corrosion resistance of $[(Fe_{0.75}Mn_{0.25})Ni_{12}]Cu_{30.3}$ alloy. The corrosion rate decreases with the increase of the Cr contents up to $x = 0.15$, followed by an increasing trend. Therefore, the $[(Fe_{0.6}Mn_{0.25}Cr_{0.15})Ni_{12}]Cu_{30.3}$ alloy possess the best corrosion-resistance. The corrosion rate was 0.0008 μm/h after 240 h, which corresponded to a corrosion rate of less than 0.007 mm/year. The corrosion rate of Cupronickel(C71500) under these conditions is approximately 0.02 mm/year [15]. The appropriate Cr additions can therefore reinforce the corrosion resistance significantly.

5. Conclusions

A composition formula $[M_{1/13}Ni_{12/13}]_{30}Cu_{70}$ are pointed out for M = (Cr, Mn, Fe) alloyed $Cu_{70}Ni_{30}$ (at.%) alloys by using a cluster-based stable solid solution model, where the M-centered and 12-Ni shelled clusters are imbedded in a Cu matrix. The designed alloys, formulated by $[(Fe_{0.75-x}Mn_{0.25}Cr_x)_1Ni_{12}]Cu_{30.3}$, all show superior corrosion resistance, and in particular $[(Fe_{0.6}Mn_{0.25}Cr_{0.15})_1Ni_{12}]Cu_{30.3}$ has the best corrosion resistance in 3.5% NaCl aqueous solution.

Acknowledgements

This project is supported by the National Science Foundation of China (No. 50901012) and by the National Basic Research Program of China (No. 2007CB613902).

References

[1] A.J. Sedriks, Advanced materials in marine environments, Mater. Perf. 33 (1994) 56–63.
[2] C. Pearson, Role of iron in the inhibition of corrosion of marine heat exchangers, Br. Corros. J. 7 (1972) 61–682.
[3] L.J.P. Drolenga, F.P. Ijsseling, B.H. Kolster, The influence of alloy composition and microstructure on the corrosion behaviour of Cu–Ni alloys in seawater, Mater. Corros. 34 (1983) 167–178.
[4] K.D. Efird, The synergistic effect of Ni and Fe on the seawater corrosion of copper alloy, Corrosion 33 (1977) 347–351.
[5] G.L. Bailey, Copper-nickel iron alloys resistant to sea-water corrosion, J. Inst. Metals 79 (1951) 243–292.
[6] L.J. Swartzendruber, L.H. Bennett, The effect of Fe on the corrosion rate of copper rich Cu–Ni alloys, Scripta Metall. 2 (1968) 93–97.
[7] D.B. Anderson, Chromium modified copper–nickel alloys for improved seawater impingement resistance, J. Eng. Power Trans. ASME 92 (1973) 132–135.
[8] C. Dong, Q. Wang, J.B. Qiang, Y.M. Wang, N. Jiang, G. Han, Y.H. Li, J. Wu, J.H. Xia, From clusters to phase diagrams: composition rules of quasicrystals and bulk metallic glasses, J. Phys. D: Appl. Phys. 40 (2007) R273–R291.
[9] C. Dong, W.R. Chen, Y.G. Wang, J.B. Qiang, Q. Wang, Y. Lei, Calvo-Dahlborg, M. Dubois, Formation of quasicrystals and metallic glasses in relation to icosahedral clusters, J. Non-Cryst. Solids 353 (2007) 3405–3411.
[10] J. Zhang, Q. Wang, Y.M. Wang, C.Y. Li, L.S. Wen, C. Dong, Revelation of solid solubility limit Fe/Ni = 1/12 in corrosion-resistant Cu-Ni alloys and relevant cluster model, J. Mater. Res. 45 (2010) 328–336.
[11] J. Zhang, Q. Wang, Y.M. Wang, C. Dong, Study on the cluster-based model of $Ni_{30}Cu_{70}$ solid solution with Fe and Mn addition and its corrosion resistance, Acta Metall. Sinica 45 (2009) 1390–1395.
[12] A. Takeuchi, A. Inoue, Calculations of mixing enthalpy and mismatch entropy for ternary amorphous alloys, Mater. Trans. JIM 41 (2000) 1372–1378.
[13] A. Laachach, A. Srhiri, C. Fiaud, A. Benbachir, Br. Corros. J 36 (2001) 136–142.
[14] S.J. Yuan, S.O. Pehkonen, Surface characterization and corrosion behavior of 70/30 Cu-Ni alloy in pristine and sulfide-containing simulated seawater, Corros. Sci. 49 (2007) 1276–1304.
[15] R.F. North, M.J. Pryor, The influence of corrosion product structure on the corrosion rate of Cu–Ni alloys, Corros. Sci. 10 (1970) 297–311.